Investigation of the effects of autorotative flare index variation on helicopter flight dynamics in autorotation

Scaramuzzino, Paolo; Pavel, Marilena; Pool, Daan; Stroosma, Olaf; Quaranta, Giuseppe; Mulder, Max

Publication date
2019

Document Version
Final published version

Published in
45th European Rotorcraft Forum 2019, ERF 2019

European Rotorcraft Forum

INVESTIGATION OF THE EFFECTS OF AUTOROTATIVE FLARE INDEX VARIATION ON HELICOPTER FLIGHT DYNAMICS IN AUTOROTATION

Paolo F. Scaramuzzino[1,2], Marilena D. Pavel[1], Daan M. Pool[1], Olaf Stroosma[1], Giuseppe Quaranta[2], and Max Mulder[1]

[1]Delft University of Technology (The Netherlands)
{p.f.scaramuzzino, m.d.pavel, d.m.pool, o.stroosma, m.mulder}@tudelft.nl

[2]Politecnico di Milano (Italy)
{paolofrancesco.scaramuzzino, giuseppe.quaranta}@polimi.it

Abstract

Autorotation is a flight condition whereby the engine of a helicopter is no longer supplying power to the main rotor system, which is driven solely by the upward flow of the air moving through the rotor. For helicopters, autorotation is a common emergency procedure performed by pilots to safely land the vehicle in the event of a power failure or tail-rotor failure. In the classic analysis of dynamic stability of helicopters in powered flight, it is common practice to neglect the effect of variation of rotor angular velocity, as the rotorspeed is constant. However, this assumption is no longer justified in case of autorotative flight. Therefore, the rotorspeed becomes an additional degree-of-freedom in autorotation, giving rise to a new stability mode that couples with classical rigid-body modes. The present paper aims at understanding the role of the rotorspeed degree-of-freedom in modifying the stability characteristics in autorotation of rotor systems with different autorotative flare indexes. Results show that the helicopter dynamics are considerably affected in autorotation as a consequence of the fact that the rotorspeed degree of freedom couples with the heave subsidence mode. Therefore, autorotation requires a different control strategy by the pilot and should not be mistakenly considered only as an energy management task. Furthermore, the autorotative flare index, used to characterize the autorotative performance during the preliminary design phase of a new helicopter, provides only energy information. Indeed, this paper demonstrates that high values of this index, representative of good autorotative performance in terms of available energy over required energy, may lead to degraded stability characteristics of the helicopter in autorotation.

1. INTRODUCTION

Autorotation is a flight condition in which the rotation of the rotor is sustained by the airflow, rather than by means of engine torque applied to the shaft. Helicopter pilots use autorotation following partial or total power failure, in order to reach the closest suitable landing site. In this condition, the energy stored in the rotor is preserved at the expense of the helicopter's potential energy (altitude). This means that the helicopter can sustain autorotation only by means of descending flight.

It has been common practice in analyzing dynamic stability of helicopters in powered flight, to neglect the effect of variation of rotor angular velocity. Indeed, the vast majority of helicopters keep a constant rotorspeed (rpm) during flight. This function is fulfilled by the governor, which measures and regulates the speed of the engine. However, this assumption is no longer justified in case of autorotative flight where the governor is disengaged and the pilot takes over the task of controlling the rotor rpm directly. Power off limits are usually between 85% and 110% of the nominal rpm[1], such that the rotor can still produce enough thrust without the risk of loss of control or structural damage. Therefore, the rotorspeed becomes an additional degree-of-freedom (DOF) in autorotation. There is little substantial literature about the analysis of the poten-

tial impact of this additional degree-of-freedom on helicopter flight dynamics in autorotation. Nikolsky and Seckel[2–4] developed an analysis of the effects of autorotation phenomena on helicopter flight dynamics in both vertical and forward translation. This work dates back to the 1950s. More recent work was carried out by Houston[5–7], who mainly focused on autogyros, for which autorotation is the normal mode of operation.

The present paper aims at understanding how the rotorspeed degree-of-freedom impacts the classical rigid body modes, and therefore the handling qualities in autorotation. This is achieved by comparing the eigenvalues of a 3-DOF longitudinal model in level flight with those of a 4-DOF (3-DOF longitudinal + RPM) model in steady descent during autorotation, both representative of the Bo-105 helicopter. Moreover, the paper investigates the effects of autorotative flare index variations on helicopter stability in autorotation. There are many possible alternatives to express the autorotative characteristics of a helicopter[8–10]. The definition adopted in this paper considers the autorotation index as the ratio between the available energy (energy stored in the rotor) and the energy required to arrest the rate of descent of the helicopter prior to ground contact (proportional to weight and disk loading). This index has been chosen because it has shown to be a reasonably reliable indicator of the relative ease of making successful autorotative landings[10]. Every design parameter involved in the calculation of the autorotative flare index has been varied in order to study the sensitivity of the helicopter's eigenmodes to changes in the autorotation index, and therefore understand whether any of these parameters has a strong impact on the stability of the system.

Pilots will need to adjust their control strategy based on the helicopter dynamics they control. As a consequence, different handling characteristics may put a different level of workload on the pilot to accomplish the task. This may also have implications for autorotation training from a safety perspective. For instance, during in-flight training of novice pilots it is desirable to adopt a progressive difficulty approach, starting in a low resource demanding configuration and then transitioning to a more challenging one. During simulator training instead, starting the training in the highest resource demanding setting may provide the pilot with more robust and flexible flying skills that can then be transferred to the actual helicopter[11]. The present study sets the basis for future work on autorotation training in flight simulators.

The paper is structured as follows. First, in Section 2, the proposed methodology to analyze helicopter stability in autorotation is introduced. Then the obtained results are presented in Section 3. Finally a discussion is included in Section 4 and conclusions are drawn in Section 5.

2. METHODOLOGY

The helicopter dynamics in autorotation is analyzed in terms of stability characteristics of its modes of motion. Thirty-two different configurations have been considered (Tab. 1). They were obtained by individually varying some basic design parameters of the baseline helicopter to get realistic values of the autorotative flare index, a metric that helps to size the rotor during preliminary design studies. The baseline helicopter is the Bo-105 and its data were taken from Padfield[12]. The procedure followed to select these configurations is extensively explained in Sec. 2.1.

The comparison of the dynamic behavior of the different configurations will provide insight into which basic design parameters involved in the calculation of the autorotative index affect helicopter's stability in autorotation the most, making it more difficult to control.

2.1. Autorotation Index

The preliminary design phase of a new helicopter involves a trade-off procedure between performance in hover and in forward-flight[13]. Different constraints should be taken into account in order to avoid infeasible solutions. Among all the design requirements, also performance in autorotation plays a crucial role. Indeed, the ability of the pilot to land safely after total power failure does not depend only on his skills, but also on the physical characteristics of the helicopter. This consideration leads to the desire to quantify the autorotative characteristics of a given helicopter tracing these back to its basic design parameters. Since the execution of the whole autorotation manoeuvre can be interpreted as an energy management task, a suitable index for measuring autorotative performance should take into account the kinetic energy stored in the rotor.

Although several types of metrics can be defined[8,9], the *autorotation index* is basically a stored energy factor. The index used in this paper (Eq. (1)) was derived by Fradenburgh[10] from simple momentum relations assuming that the helicopter is initially in a steady descent in autorotation, so that the problem becomes reducing the rate of descent prior to touch-down as much as possible.

$$AI = \frac{I_R \Omega^2}{2WDL} \tag{1}$$

Table 1: Configuration test matrix.

Design parameter	Autorotative flare index AI (ft^3/lb)	Blade chord c (m)	Main rotor radius R (m)	Main rotor speed Ω (rad/s)	Helicopter weight W (kg_f)
Blade chord	5	0.0578	4.91	44.4	2200
	10	0.1157			
	15	0.1735			
	20	0.2313			
	25	0.2892			
	30	0.3470			
	35	0.4049			
	40	0.4627			
Main rotor radius	5	0.2700	3.61	44.4	2200
	10		4.14		
	15		4.49		
	20		4.76		
	25		4.98		
	30		5.16		
	35		5.32		
	40		5.47		
Main rotor speed	5	0.2700	4.91	20.6	2200
	10			29.1	
	15			35.6	
	20			41.1	
	25			46.0	
	30			50.3	
	35			54.4	
	40			58.1	
Helicopter weight	5	0.2700	4.91	44.4	4753
	10				3361
	15				2744
	20				2377
	25				2126
	30				1941
	35				1797
	40				1681

The autorotative flare index (Eq. (1)) can be interpreted as the ratio between the available energy (rotor kinetic energy $I_R\Omega^2/2$, where I_R is the polar moment of inertia of the rotor system and Ω is the rotor RPM) and the energy required to stop the rate of descent of the helicopter (proportional to the helicopter weight W and the disk loading DL). Thus, a high value of the index is desirable. In order to compare the values of this index for various helicopters, it is convenient to plot the parameter proportional to rotor kinetic energy per unit gross weight $I_R\Omega^2/2/W$ versus disk loading DL. This graphical form is adopted in Fig. 1, where an overview of typical values of the autorotation index is given. Straight lines through the origin correspond to constant values of the index. Several helicopters have been considered and all of them have an autorotative index between 5 and 40 ft^3/lb.
Some of the parameters in Eq. (1) are closely related, hence it is not possible to isolate the contribution of each of them to the overall autorotative perfor-

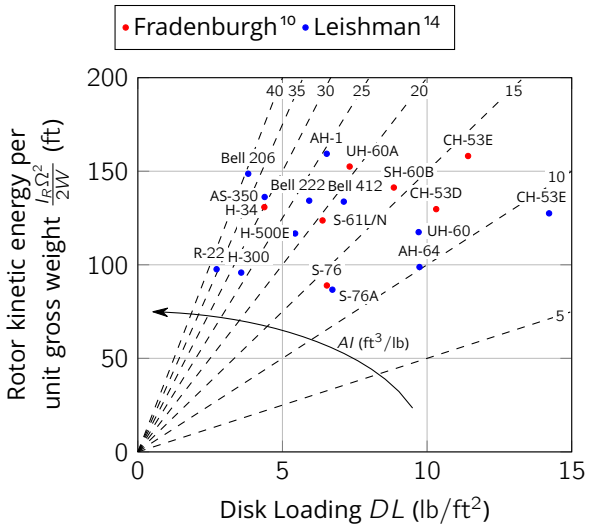

Figure 1: Autorotative indices for several helicopters at standard sea level conditions (revised from Fradenburgh[10] and Leishman[14]).

mance. For this reason, an approximate form of the autorotation index of Eq. (1) has been derived.
For this approximation it is assumed that:

- the main rotor blade mass density ρ_b is uniform, so that its mass can be expressed as:

$$m_b \simeq \rho_b th R c \tag{2}$$

where th is the blade airfoil mean thickness, c is the blade mean chord and R is the main rotor radius;

- the main rotor blade flap moment of inertia I_β can be approximated with that of a thin rod:

$$I_\beta \simeq m_b \frac{R^2}{3} = \rho_b th \frac{c R^3}{3} \tag{3}$$

- the polar inertia of the rotor system I_R can be approximated as the product between the number of blades on main rotor N_b and the main rotor blade flap moment of inertia I_β:

$$I_R \simeq N_b I_\beta \simeq N_b \rho_b th \frac{c R^3}{3} \tag{4}$$

With these assumptions and using the definition of disk loading DL:

$$DL = \frac{W}{\pi R^2} \tag{5}$$

the autorotation index of Eq. (1) can be approximated as:

$$AI \simeq \frac{\pi}{6} N_b \rho_b th \frac{c R^5 \Omega^2}{W^2} \tag{6}$$

Seven independent design parameters have been identified (N_b, ρ_b, th, c, R, Ω and W). However, the number of blades on the main rotor N_b, blade mass density ρ_b, and blade airfoil mean thickness th were fixed to the baseline value, reducing by three the number of independent design parameters.
Each of the four design parameters of Eq. (6) was varied individually to get eight different values of autorotation index, ranging from 5 to 40 $\mathrm{ft}^3/\mathrm{lb}$, for a total of 32 configurations, that are summarized in Tab. 1 and shown graphically in Fig. 2. Please note that some of the configurations are not physically feasible. Indeed, these configurations do not correspond to existing helicopters, but they are hypothetical variants of the Bo-105 helicopter with different autorotation indexes.

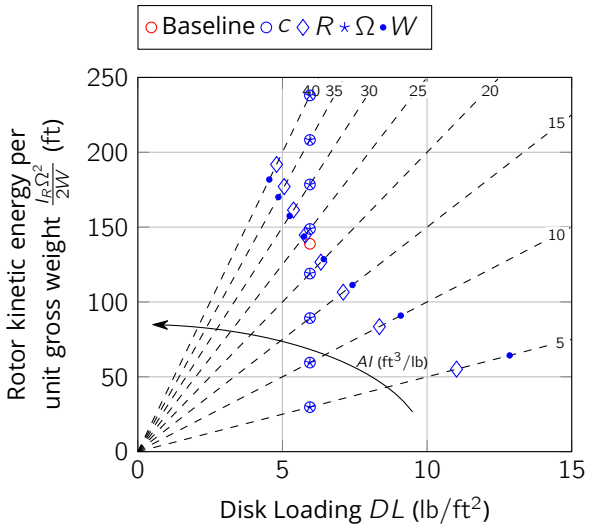

Figure 2: Autorotative indices for the helicopter's configurations listed in Tab. 1 at standard sea level conditions.

2.2. Natural Modes of Motion

It is common practice in studying the stability and control of both fixed- and rotary-wing aircraft to linearize the equations of motion around an equilibrium point and evaluate the natural modes of motion of the equivalent linear system. Indeed, linearization allows for interpreting the helicopter motion as a linear combination of natural modes, each having its own unique frequency, damping and distribution of the response states. Thus, the stability of the motion caused by small disturbances from a trim condition is strictly related to the stability of the individual modes.
The result of the linearization procedure is a state-space model of the form of Eq. (7).

$$\begin{cases} \delta \dot{\boldsymbol{x}}(t) = \mathbf{A}\, \delta \boldsymbol{x}(t) + \mathbf{B}\, \delta \boldsymbol{u}(t) \\ \delta \boldsymbol{x}(t_0) = \delta \boldsymbol{x}_0 \end{cases} \tag{7}$$

According to Lagrange's formula for linear time-invariant systems (Eq. (8)), the motion of the state $\delta \boldsymbol{x}$ is made of two different contributions: the natural response $\delta \boldsymbol{x}_n$ (also known as free or initial response) and the forced response $\delta \boldsymbol{x}_f$.

$$\begin{aligned} \delta \boldsymbol{x}(t) &= \delta \boldsymbol{x}_n(t) + \delta \boldsymbol{x}_f(t) = \\ &= \overbrace{\exp\left[\mathbf{A}(t - t_0)\right] \delta \boldsymbol{x}_0}^{\text{Natural response}} + \\ &+ \underbrace{\int_{t_0}^{t} \exp\left[\mathbf{A}(t - \tau)\right] \mathbf{B}\, \delta \boldsymbol{u}(\tau)}_{\text{Forced response}} \end{aligned} \tag{8}$$

The natural response is strictly related to the stability of the system. The eigenvectors $\boldsymbol{w}_i$ of the matrix **A**, if arranged into columns to form a square matrix **W**, satisfy Eq. (9).

$$\mathbf{W}\,\mathrm{Diag}\,(\lambda_i) = \mathbf{A}\,\mathbf{W} \tag{9}$$

where $\mathrm{Diag}\,(\lambda_i)$ is a diagonal matrix whose elements are the eigenvalues of **A**. Thus, **A** can be expressed as in Eq. (10).

$$\mathbf{A} = \mathbf{W}\,\mathrm{Diag}\,(\lambda_i)\mathbf{W}^{-1} \tag{10}$$

where the columns of **W** are referred to as right eigenvectors and those of $\mathbf{W}^{-1}$ as left eigenvectors Substituting Eq. (10) in Eq. (8), the natural response can be obtained from Eq. (11).

$$\delta\boldsymbol{x}_n\,(t) = \mathbf{W}\,\mathrm{Diag}\left[e^{\lambda_i(t-t_0)}\right]\mathbf{W}^{-1}\,\delta\boldsymbol{x}_0 \tag{11}$$

In order to isolate the contribution of each mode to the natural response, index notation is used, leading to Eq. (12).

$$\delta\boldsymbol{x}_n\,(t) = \sum_{i=1}^{n} \boldsymbol{w}_i\,\boldsymbol{v}_i^{\mathrm{H}}\delta\boldsymbol{x}_0\,e^{\lambda_i(t-t_0)} \tag{12}$$

where $\boldsymbol{v}_i^{\mathrm{H}}$ represents the i-th row of $\mathbf{W}^{-1}$ and H indicates the conjugate transpose (also known as Hermitian transpose). According to Eq. (12), the natural response of the system is given by the linear combination of the individual contributions of each mode of motion. The distribution of the response states due to each mode is specified by the corresponding eigenvector, while the information about the time evolution is contained in the respective eigenvalue. The linear approximation that allows this interpretation is extremely powerful in enhancing physical understanding of vehicle's complex motions.
In order to apply this approach to gain insight into the physics of the helicopter dynamic behaviour in autorotation, it is worth to divide the autorotation manoeuvre in three phases: steady descent, cyclic flare and rotation and collective flare[15] (points 2, 3 and 4 of Fig. 3, respectively). Since steady descent in autorotation is an equilibrium condition, it is possible to linearize the equations of motion around this condition and study the stability of the linearized system by analyzing the eigenvalues of the state matrix. In order to understand which design parameters, involved in the calculation of the autorotative index, mostly affect the helicopter's stability in steady autorotative descent, the eigenvalues of the different rotor configurations at the typical autorotative speed of 60 kn are compared.

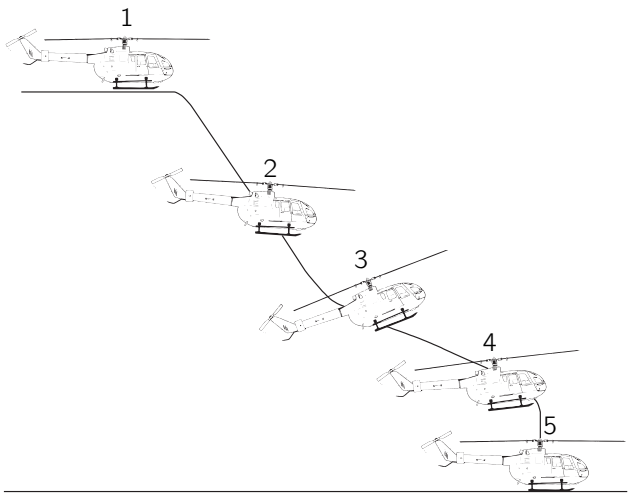

Figure 3: Autorotation phases (1: level flight, 2: steady descent, 3: cyclic flare, 4: rotation and collective flare, 5: touch-down).

3. RESULTS

This section is split in two parts. The goal of the first part is to show the effects of the rotorspeed degree of freedom on classical rigid-body modes. This is achieved by comparing the eigenvalues of a 3-DOF longitudinal model in level flight with those of a 4-DOF (3-DOF longitudinal + RPM) model in steady descent during autorotation. Both models are representative of the Bo-105 helicopter. The second part focuses on the effects of some of the basic design parameters involved in the calculation of the autorotative flare index on the helicopter's stability characteristics in autorotation. Details about the flight dynamics model are summarized in Appendix A.

3.1. Effect of RPM on Rigid-Body Modes

3.1.1. Evolution of the Eigenvalues with Forward Speed

Fig. 4 shows a comparison between the root locus in level flight (Fig. 4a, 4c and 4e) and steady descent in autorotation (Fig. 4b, 4d and 4f) for the baseline helicopter. The root loci are parametrized with forward speed, showing the evolution of each mode from low-speed flight to 140 kn. Steady descent in autorotation is a condition in which the helicopter is descending at a constant rate of descent, whose value is such that the rotor torque is zero[15]. This means that also the rate of descent changes with forward speed. These values are shown in Fig. 4d and 4f for three points (minimum speed, speed for minimum descent rate and maximum speed).

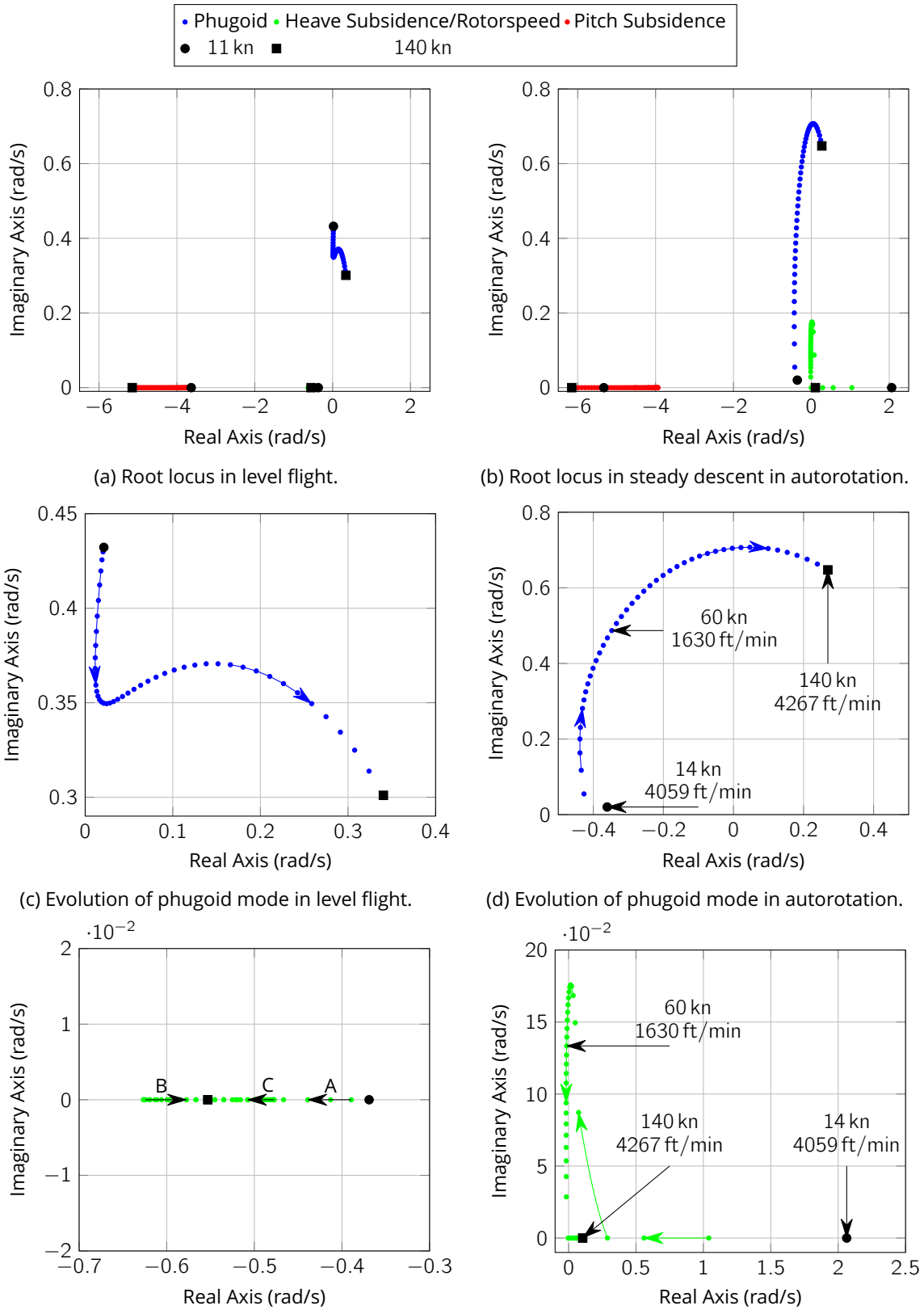

(a) Root locus in level flight.

(b) Root locus in steady descent in autorotation.

(c) Evolution of phugoid mode in level flight.

(d) Evolution of phugoid mode in autorotation.

(e) Evolution of heave subsidence mode in level flight.

(f) Evolution of heave/rotorspeed mode in autorotation.

Figure 4: Comparison between root loci in level flight and steady descent in autorotation for the baseline helicopter as a function of forward speed at standard sea level conditions.

The dynamic behavior of the helicopter in the two flight conditions is substantially different. In steady descent in autorotation, the rotorspeed mode and the heave subsidence are aperiodic modes at very low and very high speeds, whereby the former is unstable and the latter is stable. At intermediate speeds, they couple together, giving rise to a couple of complex conjugate poles (Fig. 4f) that is unstable only at low forward speeds. The phugoid is also affected by the rotorspeed mode: it becomes unstable only at high speeds (Fig. 4d). The pitch subsidence mode instead is almost unaffected by the addition of the rotorspeed state.
Thus, the rotorspeed degree of freedom has a strong influence on the classical rigid-body modes. In order to gain more insight into the dynamic characteristics of the baseline helicopter in steady descent in autorotation, let us consider the typical autorotative speed of $60\,\mathrm{kn}$. Tab. 2 shows a comparison of eigenvalues, frequency and damping characteristics at $60\,\mathrm{kn}$ ground speed between level flight and steady descent in autorotation. The phugoid mode, which is unstable and lightly damped in level flight (time to double of approximately $48\,\mathrm{s}$), becomes stable and highly damped in steady autorotation (time to halve of approximately $2\,\mathrm{s}$). The heave subsidence instead, which is stable and aperiodic in level flight (time to halve of approximately $1\,\mathrm{s}$), couples with the rotorspeed degree of freedom, giving rise to a couple of stable and lightly damped periodic poles in steady autorotation (time to halve of approximately $48\,\mathrm{s}$). The pitch subsidence slightly moves toward the left-hand side of the complex plane, but overall does not change significantly.

3.1.2. Analysis of the Eigenvectors at 60 knots

Modes in steady descent in autorotation cannot be easily matched with modes in level flight just by looking at the corresponding eigenvalues. Their identification is based on the analysis of the corresponding eigenvectors by means of a comparison with the eigenvectors in level flight. Indeed, we expect a similar behavior in terms of states' participation for equivalent modes in the two flight conditions. In Fig. 5a and 5b, the eigenvector of the phugoid mode of the Bo-105 flying at $60\,\mathrm{kn}$ ground speed is illustrated for level flight and steady descent in autorotation, respectively. The modal content of all the state vector components has been included. Angular quantities and angular rates in the eigenvectors are presented in deg and $\mathrm{deg/s}$, respectively (except for the rotorspeed degree of freedom that is presented in $\mathrm{rad/s}$) in order to be able to catch their contribution with respect to translational rates, that are shown in $\mathrm{m/s}$. Because the phugoid mode is oscillatory, each component has a magnitude and a phase, making polar plots ideal to represent its eigenvector. In level flight (Fig. 5a), the pitch rate is roughly in quadrature with the pitch angle (they are not exactly in quadrature because the mode is damped). Indeed, when the pitch rate is zero, the pitch angle has a maximum or a minimum, being the pitch rate the time derivative of the pitch angle. Moreover, the pitch rate is roughly in phase with the heave velocity and with the surge velocity. This means that when the pitch rate is zero, also heave and surge velocities are zero and according to Eq. (13) and (14), when the pitch angle reaches a maximum ($\delta\theta > 0$), the helicopter is climbing ($\delta V_{vert} = \delta\theta\, V_{fwd_{eq}} > 0$) and when it reaches a minimum ($\delta\theta < 0$), the helicopter is descending ($\delta V_{vert} = \delta\theta\, V_{fwd_{eq}} < 0$).

$$\begin{aligned}(13)\quad \delta V_{fwd} &= \delta u \cos\Theta_{eq} + \delta w \sin\Theta_{eq} + \\ &- \delta\theta\,(U_{eq}\sin\Theta_{eq} - W_{eq}\cos\Theta_{eq}) = \\ &= \delta u \cos\Theta_{eq} + \delta w \sin\Theta_{eq} - \delta\theta\, V_{vert_{eq}}\end{aligned}$$

$$\begin{aligned}(14)\quad \delta V_{vert} &= \delta u \sin\Theta_{eq} - \delta w \cos\Theta_{eq} + \\ &+ \delta\theta\,(U_{eq}\cos\Theta_{eq} + W_{eq}\sin\Theta_{eq}) = \\ &= \delta u \sin\Theta_{eq} - \delta w \cos\Theta_{eq} + \delta\theta\, V_{fwd_{eq}}\end{aligned}$$

The situation is highly similar in steady autorotation (Fig. 5b). The main difference is given by the presence of the rotorspeed state, which is actually roughly in phase with the pitch angle. This is an expected result in autorotation, because pitching up allows the airflow to pass through the rotor from below, speeding it up. Furthermore, in steady descent in autorotation there is a non-zero vertical speed ($V_{vert_{eq}} < 0$), meaning that when the pitch angle reaches a maximum ($\delta\theta > 0$), the helicopter is accelerating with respect to the ground ($\delta V_{fwd} = -\delta\theta\, V_{vert_{eq}} > 0$) and decreasing its rate of descent ($\delta V_{vert} = \delta\theta\, V_{fwd_{eq}} > 0$) and when it reaches a minimum ($\delta\theta < 0$), the helicopter is decelerating with respect to the ground ($\delta V_{fwd} = -\delta\theta\, V_{vert_{eq}} < 0$) and increasing its rate of descent ($\delta V_{vert} = \delta\theta\, V_{fwd_{eq}} < 0$).
The same polar representation has been used to compare the heave subsidence mode in level flight (Fig. 5c) with the combined heave/rotorspeed mode in steady autorotation (Fig. 5d). Although the heave subsidence mode in level flight is non-oscillatory and a simple bar plot would have been sufficient to analyze its eigenvector, the change in the nature of this mode to oscillatory when in steady autorotation makes polar plots the best choice to achieve a fair comparison.

Table 2: Eigenvalues, frequency and damping characteristics at 60 kn for the baseline helicopter - Comparison between level flight and steady descent in autorotation.

Mode	Level flight				Steady descent in autorotation			
	λ (rad/s)		ω_n (rad/s)	ξ (-)	λ (rad/s)		ω_n (rad/s)	ξ (-)
	$\Re(\lambda)$	$\Im(\lambda)$			$\Re(\lambda)$	$\Im(\lambda)$		
Phugoid	0.0212	−0.3497	0.3503	−0.0605	−0.3472	−0.4869	0.5980	0.5806
	0.0212	0.3497	0.3503	−0.0605	−0.3472	0.4869	0.5980	0.5806
Heave/ Rotorspeed	−0.6197	0.0000	0.6197	1.0000	−0.0146	−0.1334	0.1342	0.1087
					−0.0146	0.1334	0.1342	0.1087
Pitch sub.	−4.0783	0.0000	4.0783	1.0000	−4.2596	0.0000	4.2596	1.0000

In level flight (Fig. 5c), the pitch rate is in antiphase with the pitch angle. This is explained by the fact that the response of the system is strictly monotone (i.e., the heave subsidence eigenvalue is real, therefore the response follows an exponential) and convergent to zero (i.e., the heave subsidence eigenvalue is stable), hence the pitch rate, that is the time derivative of the pitch angle, needs to be opposite in sign with respect to the pitch angle (i.e., if one is strictly decreasing to zero from positive values, the other one is strictly increasing to zero from negative values). Furthermore, the pitch rate is in phase with the heave velocity and in antiphase with the surge velocity. However, the magnitude of the heave velocity is much higher than that of the other states, meaning that the motion is a rapid variation of the heave velocity.

The situation slightly changes in steady autorotation (Fig. 5d), whereby the combined heave/rotorspeed mode is oscillatory. The pitch rate is roughly in quadrature with the pitch angle (they are not exactly in quadrature because the mode is damped). Indeed, when the pitch rate is zero, the pitch angle has a maximum or a minimum, being the pitch rate the time derivative of the pitch angle. Moreover, the pitch rate is roughly in phase with the rotorspeed, meaning that when the helicopter pitches up the rotorspeed increases and when it pitches down the rotorspeed decreases, as expected. The rotorspeed state is roughly in antiphase with the heave velocity and in phase with the surge velocity. This is also expected, since when the rotor speeds up, it generates more thrust, hence reducing the rate of descent and increasing the forward speed, as long as the rotor is tilted forward.

A bar plot has been used to compare the pitch subsidence mode between level flight and steady autorotation (Fig. 5e). Indeed, the pitch subsidence mode is non-oscillatory in both flight conditions.

It can be noticed that state participation is similar for both flight conditions. Apart from the presence of the rotorspeed degree of freedom, which was neglected in level flight, the only difference between the two flight conditions is related to the phase of the surge velocity. The same explanation adopted for the heave subsidence can also be used for the pitch subsidence. Indeed, the pitch rate is in phase with the rotorspeed, meaning that when the helicopter pitches up the rotorspeed increases and when it pitches down the rotorspeed decreases. When the rotor speeds up, it generates more thrust, hence reducing the rate of descent and increasing the forward speed, as long as the rotor is tilted forward. This is the reason why the rotorspeed state is in antiphase with the heave velocity and in phase with the surge velocity.

3.2. Effect of Autorotative Index Design Parameters on Helicopter Stability Characteristics in Autorotation

The stability characteristics of the set of helicopter configurations defined in Sec. 2.1 have been evaluated and are shown in Fig. 6. This set of configurations has been divided into four subsets, each of which is related to a specific design parameter (see Tab. 1). Fig. 6a, 6b, 6c and 6d show the sensitivity of the modes to changes in the main rotor blade chord c, main rotor radius R, main rotor RPM Ω and helicopter weight W, respectively.

For every subset of configurations, it can be noticed that increasing the autorotative flare index has:

- positive effects on the stability of the phugoid mode;
- negative effects on the stability of the pitch subsidence. However, the pitch subsidence remains stable;
- negative effects on the stability of the heave/rotorspeed mode, which even becomes slightly unstable for high values of the index.

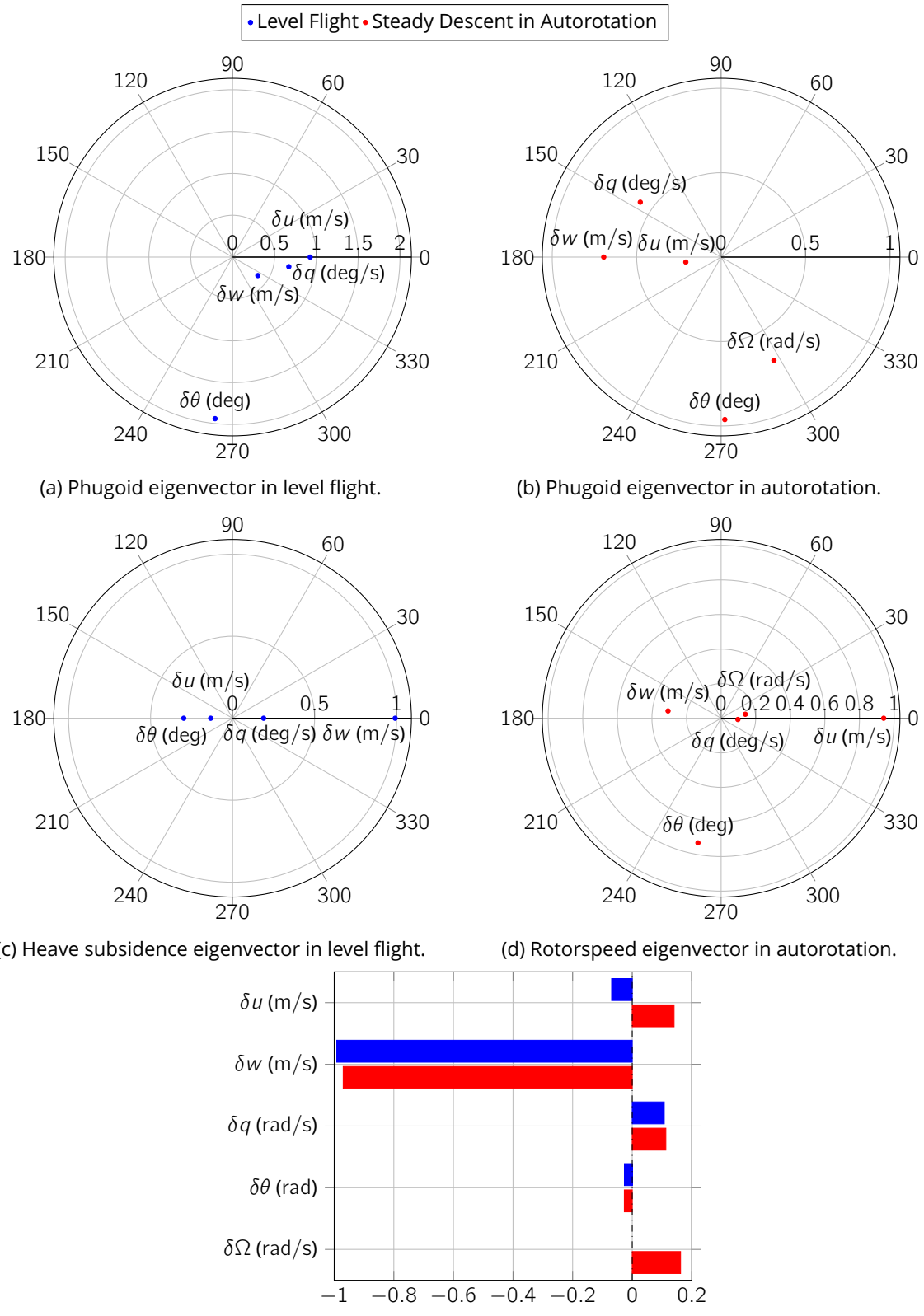

(a) Phugoid eigenvector in level flight.

(b) Phugoid eigenvector in autorotation.

(c) Heave subsidence eigenvector in level flight.

(d) Rotorspeed eigenvector in autorotation.

(e) Comparison between pitch subsidence eigenvector in level flight and in autorotation.

Figure 5: Comparison between eigenvectors in level flight and steady descent in autorotation for the baseline helicopter at 60 kn forward speed at standard sea level conditions.

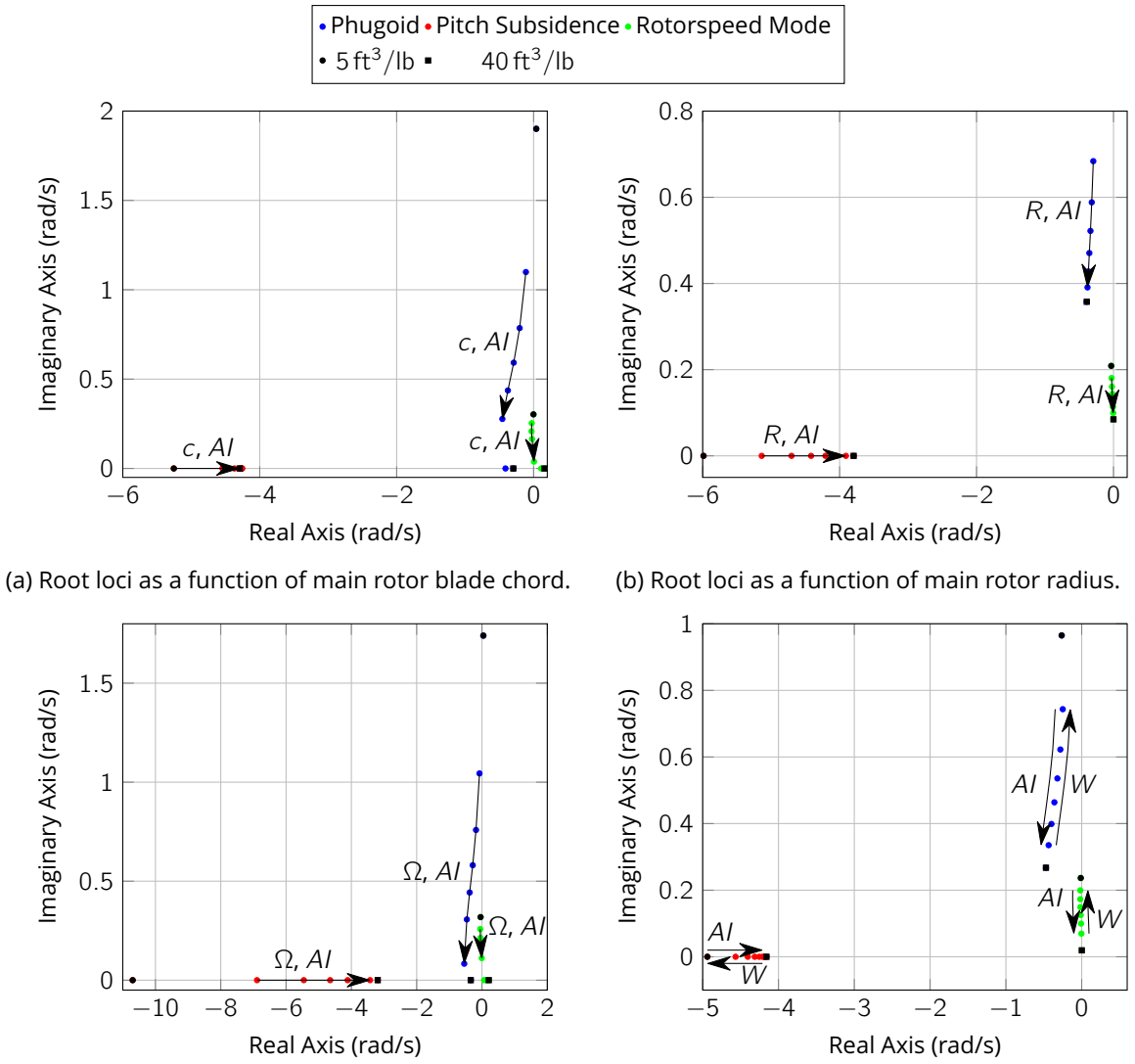

(a) Root loci as a function of main rotor blade chord.

(b) Root loci as a function of main rotor radius.

(c) Root loci as a function of main rotor RPM.

(d) Root loci as a function of helicopter weight.

Figure 6: Comparison between root loci in steady descent in autorotation for the different helicopter's configurations as a function of the autorotation index at standard sea level conditions.

3.2.1. Effects of Autorotative Index on the Phugoid Mode

These results are explained by the fact that the stability characteristics of the phugoid mode are mainly related to the speed derivative M_u. Although positive values of this derivative have a stabilizing effect, the phugoid mode becomes more stable when M_u decreases, balancing the effects of the pitch-damping derivative M_q. Indeed, the phugoid oscillation is fostered by the helicopter attempts to re-establish the equilibrium level-flight condition from which it had been disturbed. The strong coupling of u and q may lead to an unstable phugoid mode. It can be noticed from Fig. 5a and 5b that u and q are almost perfectly in phase in level flight and only roughly in phase in steady autorotation, justifying the fact that the phugoid mode becomes stable in autorotation. Increasing the autorotative flare index reduces M_u (Fig. 7a), making the phugoid mode more stable.

3.2.2. Effects of Autorotative Index on the Pitch Subsidence Mode

The stability characteristics of the pitch subsidence mode are mainly related to the pitch-damping derivative M_q. Negative values of this derivative make this mode stable. Increasing the autorotative flare index increases M_q (Fig. 7b), which makes the pitch subsidence mode less stable.

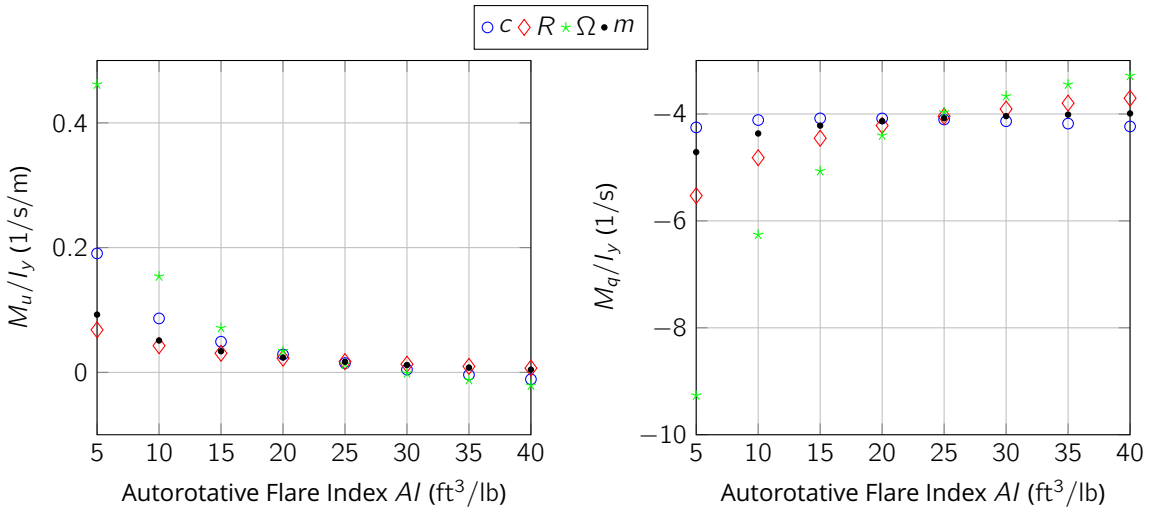

(a) Speed stability derivative M_u.

(b) Pitch-damping derivative M_q.

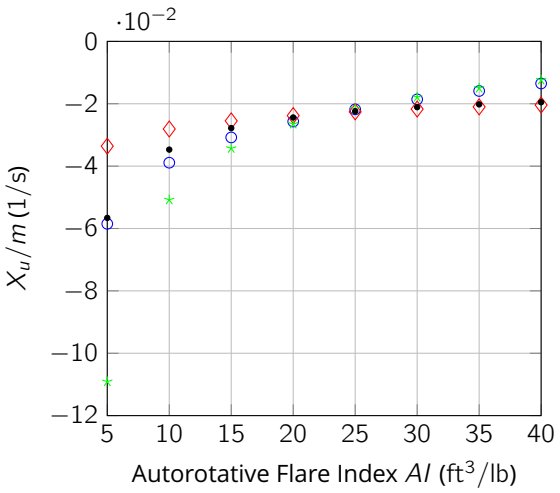

(c) Surge-damping derivative X_u.

Figure 7: Stability derivatives as a function of autorotative flare index.

3.2.3. Effects of Autorotative Index on the Heave/Rotorspeed Mode

The stability characteristics of the heave subsidence in level flight are mainly related to the heave-damping derivative Z_w. Negative values of this derivative are likely to make this mode stable. However, in autorotation, the heave subsidence couples with the rotorspeed mode, making the isolated analysis of Z_w insufficient to get insight into the stability of this mode. It can be noted from Fig. 5c and 5d that the heave velocity w is no longer the most excited state in steady autorotation, but it has been replaced by the surge velocity u. This means that the surge-damping derivative X_u plays a crucial role in the stability of the heave/rotorspeed mode in autorotation. Increasing the autorotative flare index reduces X_u (Fig. 7c), making the heave/rotorspeed mode less stable.

4. DISCUSSION

The present paper investigated the effects of the rotor RPM degree of freedom in autorotation on classical rigid-body modes. The proposed methodology relies on various assumptions (e.g., linearization and stability analysis), that make it applicable only to the steady descent part of the autorotation manoeuvre, which can be considered as a trim condition.

According to the analysis carried out, the helicopter dynamics change considerably in autorotation as the rotorspeed degree of freedom couples with the classical rigid body modes. Therefore, autorotation requires a different stabilization strategy by the pilot and should not be mistakenly considered only as an energy management task. Indeed, the results show that there are two main differences between the modes in straight level flight and those in steady

descent in autorotation for the baseline helicopter (Bo-105) considered in this study.

The first difference is that *the phugoid in autorotation becomes unstable only at high speeds*. The eigenvector analysis at the typical autorotative speed, shows that this is due to the fact that the surge velocity u and the pitch rate q are not in phase as in straight level flight. This means that the speed derivative M_u and the pitch-damping derivative M_q, whose interaction is responsible for the instability of the phugoid in straight level flight, are not coupled enough to foster the unstable phugoid oscillation.

Typically, M_u is positive (for a stabilizing contribution*) and M_q is negative (for a stabilizing contribution†) and the combination of these two opposite, yet independently stabilizing, effects causes the phugoid mode in straight level flight to be a slow interchange between kinetic energy (speed) and potential energy (altitude). Indeed, the phugoid oscillation is fostered by the helicopter attempts to re-establish the equilibrium level-flight condition from which it had been disturbed.

The second difference is that *the heave subsidence mode couples with the rotorspeed degree of freedom, giving rise to a couple of complex conjugate poles*. The eigenvector analysis at the typical autorotative speed, shows that the heave velocity w is no longer the most excited state during autorotation (as it is for straight level flight), but it has been replaced by the surge velocity u.

Both X_u and Z_w are typically negative (for a stabilizing contribution‡§) and the combination of these two effects, although independently stabilizing, is the reason that causes the heave/rotorspeed mode in steady autorotation to be a slow interchange between kinetic energy (speed) and rotational energy (rotorspeed). This phenomenon is somehow similar to what happens for the phugoid mode in level flight, even though in this case the oscillation is stable.

The present paper has also investigated whether large variations of the autorotative flare index strongly affect helicopter dynamics in autorotation, because this may have consequences on pilot control strategy and workload. The autorotative flare index is used in any helicopter development program by Sikorsky Aircraft[10] as a metric for satisfactory autorotative characteristics and, within certain constraints, it appears to be a reasonably reliable indicator of the relative ease of making successful autorotative landings. Four independent design parameters are involved in the calculation of this index: the main rotor blade chord, the main rotor radius, the rotor RPM and the helicopter weight. Each of them has been varied individually from the baseline value to get eight different values of the autorotation index, spanning from 5 to 40 $\mathrm{ft}^3/\mathrm{lb}$. This range was chosen after comparing the index for various existing helicopters.

For each of the four sub-sets of configurations, the sensitivity of the eigenvalues to changes in the autorotation index shows the same results. When the autorotative flare index increases, the stability of the phugoid mode improves, because the speed stability derivative M_u decreases. The opposite happens for the pitch subsidence (the pitch-damping stability derivative M_q increases) and for the heave/rotorspeed mode (the surge-damping stability derivative X_u increases). Thus, higher values of the autorotation index, representative of good autorotative performance in terms of available energy over required energy, do not necessarily mean better stability characteristics.

In order to gain insight into how pilots adapt their control strategy to the variation of the helicopter dynamics in autorotation and to the changes in the autorotative flare index, as a next step, a pilot-in-the-loop experiment will be conducted on the SIMONA Research Simulator at Delft University of Technology. Test pilots will be invited to perform the autorotation manoeuvre with the different helicopter's configurations analyzed in the present paper. Pilot ratings, pilot commentary and some objective performance metrics will be collected in order to validate the proposed methodology and to isolate two flyable configurations characterized by different workloads required by the pilot. The selected configurations will be then used in a quasi-transfer-of-training experiment to test whether the group of participants that starts the training in the most challenging setting develops more robust and flexible flying skills than the group that starts the training in the least demanding setting, as previous experimental evidence has shown[11].

*If u is positively perturbed from the equilibrium condition, the helicopter tends to pitch-down in order to gain forward speed. This effect is balanced by the fact that an increment in u leads to a pitch-up moment if M_u is positive.

†If q is positively perturbed from the equilibrium condition, the helicopter tends to pitch-up. This effect is balanced by the fact that an increment in q leads to a pitch-down moment if M_q is negative.

‡If u is positively perturbed from the equilibrium condition, the fuselage drag increases. Thus, X decreases balancing the increment of u.

§If w is positively perturbed from the equilibrium condition, the angle of attack increases, hence rotor thrust increases as well. Thus, Z decreases balancing the increment of w.

5. CONCLUSION

The present paper applied linear dynamics system theory to assess helicopter stability characteristics in autorotation. In order to achieve this goal, the classical system of equations describing the helicopter flight dynamics, which comprises the rigid-body degrees of freedom of the fuselage, has been augmented by the rotor torque equation. Indeed, the main difference with respect to powered flight is that in autorotation the rotor RPM becomes a true degree of freedom, because the governor is disengaged and no longer fulfils the task of keeping the rotorspeed constant. The validity of this analysis is restricted to the steady descent phase of the autorotation manoeuvre, that can be considered as a trim condition.

The results show that the helicopter dynamics are considerably affected in autorotation as a consequence of the fact that the rotorspeed degree of freedom couples with the classical rigid-body modes. Therefore, autorotation requires a different control strategy by the pilot and should not be considered only as an energy management task, as it is qualified by the autorotative flare index. Indeed, high values of the index may lead to degraded stability characteristics and hence a possibly more difficult autorotation.

Future work is necessary to validate the proposed methodology and to understand whether it can be applied to predict autorotation training outcomes in flight simulators.

ACKNOWLEDGEMENTS

This study has been carried out in the context of the European Joint Doctorate NITROS (Network for Innovative Training on Rotorcraft Safety) project, whose main goal is to enhance rotorcraft safety by addressing critical aspects of their design. This project has received fundings from the European Union's Horizon 2020 research and innovation programme under the Marie Skłodowska-Curie grant agreement N° 721920.

REFERENCES

[1] EASA. Type Certificate Data Sheet R.011 - BO105. TCDS EASA.R.011, 2017.

[2] A. A. Nikolsky and E. Seckel. An Analytical Study of the Steady Vertical Descent in Autorotatian of Single-Rotor Helicopters. NACA TN-1906, 1949.

[3] A. A. Nikolsky and E. Seckel. An Analysis of the Transition of a Helicopter from Hovering to Steady Autorotative Vertical Descent. NACA TN-1907, 1949.

[4] A. A. Nikolsky. The Longitudinal Stability and Control of Single Rotor Helicopters in Autorotative Forward Flight. Princeton University Aero. Eng. Lab. Report No. 215, 1952.

[5] S. S. Houston. Longitudinal stability of gyroplanes. *Aeronautical Journal*, 100(991):1–6, 1996.

[6] S. S. Houston. Validation of a Rotorcraft Mathematical Model for Autogyro Simulation. *Journal of Aircraft*, 37(3):403–409, 2000.

[7] S. S. Houston. Analysis of Rotorcraft Flight Dynamics in Autorotation. *Journal of Guidance, Control, and Dynamics*, 25(1):33–39, 2002.

[8] T. L. Wood. High Energy Rotor System. In *Proceedings of the AHS Annual Forum 32*, 1976.

[9] G. White, A. H. Logan, and R. Graves. An Evaluation of Helicopter Autorotation Assist Concepts. In *Proceedings of the AHS Annual Forum 38*, 1982.

[10] E. A. Fradenburgh. Technical Notes: A Simple Autorotative Flare Index. *Journal of the American Helicopter Society*, 29(3):73–74, jul 1984.

[11] H.-G. Nusseck, H. J. Teufel, F. M. Nieuwenhuizen, and H. H. Bülthoff. Learning System Dynamics: Transfer of Training in a Helicopter Hover Simulator. In *Proceedings of the AIAA Modeling and Simulation Technologies Conference and Exhibit*, Honolulu, Hawaii, 2008.

[12] G. D. Padfield. *Helicopter Flight Dynamics: The Theory and Application of Flying Qualities and Simulation Modelling*. Blackwell Publishing Ltd, Oxford, UK, second edition, 2007.

[13] W. Johnson. *Helicopter Theory*. 1994.

[14] J. G. Leishman. *Principles of Helicopter Aerodynamics*. 2006.

[15] R. W. Prouty. *Helicopter Performance, Stability, and Control*. Krieger Publishing Company, INC., Malabar, Florida, 2002.

[16] R. T. N. Chen. Effects of Primary Rotor Parameters on Flapping Dynamics. NASA/TP-1431, 1980.

[17] W. P. Rodden. Aerodynamic Influence Coefficients from Strip Theory. *Journal of the Aerospace Sciences*, 26(12):833–834, dec 1959.

[18] R. T. N. Chen. A Simplified Rotor System Mathematical Model for Piloted Flight Dynamics Simulation. NASA/TM-78575, 1979.

[19] P. D. Talbot, B. E. Tinling, W. A. Decker, and R. T. N. Chen. A Mathematical Model of a Single Main Rotor Helicopter for Piloted Simulation. NASA/TM-84281, 1982.

A. MATHEMATICAL MODEL OF THE HELICOPTER

A four-degrees-of-freedom analytical model, which consists of 3-DOFs longitudinal rigid-body dynamics and 1-DOF main-rotor angular velocity, was developed explicitly for a centre-spring equivalent main-rotor system[12] (see Eq. (15) and (16)).

$$\begin{cases} m\left(\dot{u}+qw\right)=-mg\sin\theta+X \\ m\left(\dot{w}-qu\right)=mg\cos\theta+Z \\ I_y\dot{q}=M \\ I_R\dot{\Omega}=Q \end{cases} \tag{15}$$

$$\begin{cases} X=X_{mr}+X_{fus} \\ Z=Z_{mr}+Z_{fus}+Z_{tp} \\ M=M_h+Z_{mr}x_h-X_{mr}h_h+M_{fus}+M_{tp} \\ Q=Q_e-Q_{mr} \end{cases} \tag{16}$$

Many simplifications and assumptions were made in deriving this model. The rotor blade was assumed to be rigid with linear twist only. Uniform inflow and steady-state tip-path plane dynamics were considered[16]. Both flapping and inflow angle were assumed to be small. Simple strip theory[17] was used. The reversed-flow region was ignored, and compressibility and stall effects were not considered. The main-rotor force and moment expressions match those developed by Chen et al.[18,19] if flapping hinge offset ($\epsilon = 0$), pitch-flap coupling ($\delta_3 = 0$) and tip-path plane dynamics ($\dot{a}_0$, $\dot{a}_1$, $\dot{b}_1 = 0$ and $\ddot{a}_0$, $\ddot{a}_1$, $\ddot{b}_1 = 0$) are neglected.

NOMENCLATURE

δ_3	Pitch-flap coupling	(° or rad)
ϵ	Non-dimensional flapping hinge offset	(-)
λ_i	i-th eigenvalue	(rad/s)
Ω	Main-rotor angular velocity	(rad/s)
ρ_b	Main rotor blade mass density	(kg/m^3)
θ	Fuselage pitch angle	(° or rad)
$\delta\boldsymbol{u}$	Perturbation of the input vector	
$\delta\boldsymbol{x}$	Perturbation of the state vector	
$\mathbf{A}$	State matrix	
$\mathbf{B}$	Control matrix	
$\mathbf{W}$	Right eigenvectors matrix	
$\boldsymbol{v}_i$	i-th left eigenvector	
$\boldsymbol{w}_i$	i-th right eigenvector	
a_0	Coning angle	(° or rad)
a_1	Longitudinal tilt angle	(° or rad)
AI	Autorotative flare index	(ft^3/lb)
b_1	Lateral tilt angle	(° or rad)
c	Main rotor blade chord	(m)
DL	Disk loading	(lb/ft^2)
g	Average gravitational field at sea level	(m/s^2)
h_h	Height of the rotor hub above helicopter center of gravity	(m)
I_R	Polar inertia of the rotor system	(kg m^2)
I_y	Helicopter pitch inertia	(kg m^2)
I_β	Main rotor blade flap moment of inertia	(kgm^2)
K_β	Flapping hinge restraint	(N m/rad)
M	Pitch moment	(N m)
m	Helicopter mass	(kg)
m_b	Main rotor blade mass	(kg)
M_q	Pitch-damping stability derivative	(N m s/rad)
M_u	Speed stability derivative	(N s)
N_b	Number of blades on main rotor	(-)
Q	Torque	(N m)
q	Pitch rate	(rad/s)
t	Time	(s)
th	Blade airfoil mean thickness	(m)
u	Body longitudinal speed	(m/s)
V_{fwd}	Forward speed	(m/s)
V_{vert}	Vertical speed	(m/s)
W	Helicopter weight	(kg$_f$ or N)
w	Body vertical speed	(m/s)
X	Body longitudinal force	(N)
x_h	Longitudinal position of the rotor hub behind helicopter center of gravity	(m)
X_u	Surge-damping stability derivative	(N s/m)
Z	Body vertical force	(N)
Z_w	Heave-damping stability derivative	(N s/m)

Subscripts

e	Engine
eq	Trim condition
fus	Fuselage
h	Hub
mr	Main-rotor
tp	Horizontal tailplane